# Optimization of Design Margins Allocation When Making Use of Additive Remanufacturing

5 authors, including:

Khalil Al Handawi
Université de Montréal
17 PUBLICATIONS  118 CITATIONS

Massimo Panarotto
Politecnico di Milano
77 PUBLICATIONS  605 CITATIONS

Petter Andersson
University of Gothenburg
21 PUBLICATIONS  83 CITATIONS

Isaksson Ola
Chalmers University of Technology
188 PUBLICATIONS  2,414 CITATIONS

# Optimization of Design Margins Allocation When Making Use of Additive Remanufacturing

**Khalil Al Handawi**
Postdoctoral Researcher
Mechanical Engineering
McGill University
Montreal, Canada
khalil.alhandawi@mail.mcgill.ca

**Massimo Panarotto**
Associate Professor
Industrial and Materials Science
Chalmers University of Technology
Göteborg, Sweden
massimo.panarotto@chalmers.se

**Petter Andersson**
Technology Lead for
Multidisciplinary Design Optimization
GKN Aerospace Engine Systems
Trollhättan ,Sweden
petter.andersson@gknaerospace.com

**Ola Isaksson**
Professor
Industrial and Materials Science
Chalmers University of Technology
Göteborg, Sweden
ola.isaksson@chalmers.se

**Michael Kokkolaras**∗
Associate Professor
Mechanical Engineering
McGill University
Montreal, Canada
michael.kokkolaras@mcgill.ca

*Often, coping with changing requirements results in substantial overdesign, because of the ways in which design margins are allocated at the beginning of the design process. In this paper, we present a design optimization method for minimizing overdesign using additive manufacturing. We use recently defined constituents of design margins (buffer and excess) as metrics in a design optimization problem to minimize overdesign. The method can be used to obtain a set of design decisions for different changing requirement scenarios. We demonstrate our method by means of a turbine rear structure design problem where changes in the temperature loads are met by depositing different types of stiffeners on the outer casing. The results of the case study are visualized in a tradespace, which allows for comparison between sets of optimal, flexible, and robust designs. Results show that the optimized set of design decisions balances flexibility and robustness in a cost-effective manner.*

## 1 Introduction

The development of complex engineering systems relies on the definition and communication of design requirements from original equipment manufacturers (OEMs) to compo-nent suppliers. While requirements are supposed to be clear and well-defined, they are subject to changes during the development process [1] as a result of iteration and concurrent engineering among the OEMs and the suppliers.

Manufacturers introduce substantial design margins in the early phases to cope with changes in requirements. Design margins accommodate changing requirements by providing a buffer before any change to the product is required. For example, consider a book shelf designed to sustain 90 N of load instead of the required 50 N to accommodate future changes in the operative load [2]. This strategy may result in overdesign if the 90 N load is never realized, which negatively impacts performance (e.g., through increased weight) [3,4].

An alternative approach is to design a component based on a preliminary requirement (aiming for minimal capability) and to modify it when higher requirements arise. In the previous example, this is the equivalent of designing the shelf to sustain 50 N, and modify the shelf for a 90 N load requirement should it arise. This alternative can be made possible using additive manufacturing (AM), which enables geometry modification on existing components through material deposition [5,6,7]. However, this strategy has drawbacks. If the changes in requirements are too many or unforeseen, the cost

---

∗Address all correspondence to this author.

of such modifications could overcome the cost of overdesigning the product.

We show an example of our own that is inspired by the industry to illustrate these challenges. A turbine rear structure (TRS) is a static aeroengine structural component that must sustain temperature loads as a result of the hot engine exhaust gases. These temperature loads can change during the design or in-service phases as is shown in Figure 1.

These changes are represented by the red line, hereafter defined as the requirement arc. The temperature requirement is assumed to change five times as a result of critical design reviews [8] and negotiations between the OEM and the manufacturer of the TRS. These five points are referred to as *epochs*, to resonate with tradespace exploration literature [9].

The manufacturer uses AM to cope with this requirement change in the above example. In particular, the manufacturer starts working on two different designs, A and B (hereafter defined as decision arcs). With AM, the geometry of the TRS can be initially designed to meet the lower bound of the temperature range, while depositing a stiffener on the structure as the temperature requirement changes (first epoch). However, the decisions made during the design of the stiffener's geometry may impact the capability of coping with changes without resulting in over design.

For instance, choosing the geometry of the deposition as decision arc A (wavy design concept) will allow for a design with a capability that fulfills the new requirement at the second epoch. However, further changes of this geometry (such as the one made at epoch 5) do not allow for close tracking of the requirement arc, resulting in overdesign (blue line). On the other hand, decision arc B (hatched design concept) allows for better tracking of the requirement arc. This reduces the risk for overdesign at the end of the process. However, this comes with the cost and effort of performing more depositions during the course of the development (4 instead of 2), outweighing the benefits given by this more flexible decision arc. There is a a trade-off between the flexibility that can be enabled by AM deposition and other attributes of the design (such as weight and manufacturing costs).

We aim at supporting these decisions by presenting a methodology - based on design optimization and tradespace exploration that quantifies such tradeoffs. The use of this method allows for strategic allocation of design margins into a component when requirement changes occur, to avoid overdesign.

## 2 Background

We first review change propagation research to identify potential sources of requirement changes in engineering systems. We then review a body of the literature that defines and quantifies flexibility and changeability of a design. Particular attention is given to tradespace exploration strategies, which represent a core building block of the methodology presented in this paper.

### 2.1 Change propagation

Requirements are defined during the early stages of a design project and guide decisions during the early conceptual phases of the design process. A client may alter design requirements resulting in engineering change. Design structure matrices (DSMs) can be used to model the direct dependencies between requirements due to an engineering change. Change prediction method (CPM) extends DSM approaches to include secondary interactions [10]. Second-order DSMs can capture second order interactions among requirements [11]. They are the key predictors for the outcome of engineering change and are often difficult to identify. The DSM approach is demonstrated by a practical case study of a contractual firm where engineering changes were initiated by the client [11, 12]

Multiple domain matrices (MDMs) asses change propagation in complex product systems. A product is broken down into individual components. Domain mapping matrices (DMMs) are combined with DSMs to propagate changes between different domains (requirements, change options, and components). Performance ratings are assigned to each change option to initiate the MDM analysis using expert knowledge. The components of the MDM are computed and used to update the initial performance ratings iteratively. This CPM helps designers identify those options closely associated with the anticipated requirement change [13].

We present an approach that can be useful for providing insight on how to select initial performance indicators for a CPM. The second-order DSM approach can be used to identify the most important requirements likely to effect an engineering change and reduce the set of possible requirement changes [11]. We assume a given set of possible requirement changes and use it to compute the performance ratings needed to initialize a CPM. We consider the allocation of design margins as change options in this paper.

### 2.2 Design margins

Design margins can be considered as a portion of a product's capability. Capability is defined as the set of possible values for a design parameter for which feasibility is maintained [2]. Quantifying design margins involves measuring the constituents of margins: buffer and excess. Buffer is defined as the portion of a design's capability reserved for meeting variations in a requirement. Excess is the portion of a design's capability beyond the limits within which a requirement may vary [14]. Design margins are incorporated into product design by augmenting the capability of a product to include parameter values beyond the initial ones that were intended to satisfy the requirements resulting in more excess. This can be referred to as overdesign [2]. Design margins can be managed by quantifying them explicitly to assess the cost and risk of moving to a new design solution later in a product's lifecycle or development process.

Tackett et al. calculate excess as the range of changing parameters that the product satisfies [14]. Cansler et al. use component specifications and functional flow information to quantify the excess at the interfaces between compo-
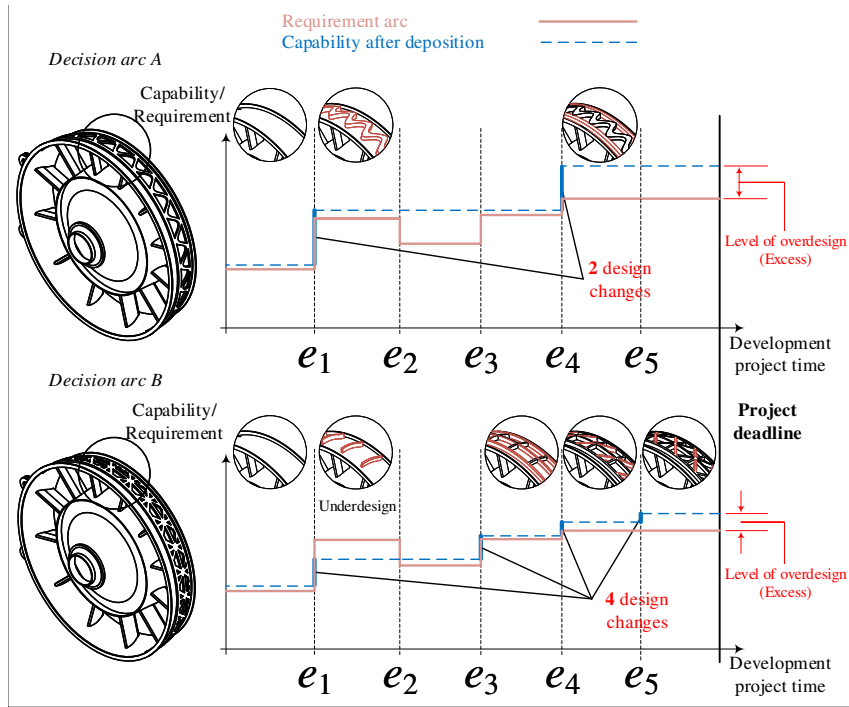
Fig. 1: Example of a product development process showcasing different decision arcs

nents [15]. Other studies define application specific capability and capacity measures [16, 17] such as the available excess for transport and storage on a ship [16]. Cross and Mulford and Villanueva et al. specify requirements in the form of probability density functions that must be met by satisfying so-called reliability levels [18, 19]. Villanueva et al attempt to optimize design margins subject to the reliability constraints.

This paper focuses on the interdependencies between changing requirements. There is a need for an approach that considers the effect of interactions between several changing requirements [2]. Furthermore, this paper focuses on the inherent uncertainty of such changing requirements. We review existing methods and metrics to quantify changeability, flexibility, and robustness to address the uncertainty surrounding requirement change.

### 2.3 Quantifying design changeability and flexibility

Design changeability is defined as the ability of a system to undergo specified changes with relative ease and efficiency [20, 21].

In design for changeability literature [22], flexibility and robustness are distinct means to include changeability in a design. Design flexibility is the ability of a design to be altered with relative ease and low cost to accommodate changes in customer requirements and operating environments [23, 24]. Robustness characterizes a product's ability to be insensitive towards changing operational environments without the need for change or modification.

There is a need for readily changeable designs that cope with changing requirements in the uncertain yet competitive market conditions that characterize the aerospace business

today.

Several studies utilize tradespace exploration strategies to quantify flexibility of a design [16, 9, 25, 26]. The main utility of tradespace exploration lies in its ability to visualize and categorize designs into sets of solutions. Viscito and Ross use Pareto optimality to extract flexible cost-efficient designs from the tradespace and plot a reduced tradespace to further analyze this reduced set [25]. One metric that is extracted from the tradespace is the filtered outdegree defined as the number of possible feasible changes that emanate from a particular design in the tradespace network [16, 25]. Changing requirements are represented as discrete time periods, called epochs during which the context, needs and requirements are stable [9]. Requirements and needs change when moving from one epoch to the next. A chain of design changes, referred to as an arc, is used to address the changing requirements [16, 25, 22, 20]. Arcs that maximize flexibility in the offered solutions are obtained using a stochastic programming problem to minimize a cost function [17].

Tradespace exploration has been successfully used in a number of studies although it has not yet been used to study the effect of design margin allocation on the flexibility of a design [26]. We define design margin components reviewed in Section 2.2 such as buffer and excess to be used as part of the multi-attribute function governing a tradespace. The use of buffer and excess as metrics for tradespace exploration studies represent the main elements of novelty of the method presented in this paper, and are introduced in the next section.

## 3 Proposed method

The study of design excess is relatively nascent. A method to strategically select design margins is required. The successful implementation of such a method requires a metric for quantifying design excess while providing a means to manage the change in requirements likely to be encountered throughout a product's lifetime or development process. Finally, the value of excess must be estimated and traded against during system design [3].

The reviewed literature does not report a method to quantify design margins (or its constituents: buffer and excess) in a multi-dimensional space by means other than intervals. The tradeoff between design robustness and flexibility has not been investigated within a tradespace exploration framework despite the abundance of studies on quantifying these aspects. Little work has been done to examine the evolutionary path of products in response to changes in their environment or requirements hence the need for an epoch-based analysis that explores product changes in a progressive manner as requirements change [3, 17].

We propose a method where we compute design reliability, capability, buffer, and excess in a multi-dimensional parameter space. We adopt the terminology of Ross et al. pertaining to arcs [22]. Each node along a decision or requirement arc represents a design alternative or requirement, respectively. We use Monte Carlo simulation to chain multiple requirements probability density functions (PDFs) together to generate a requirement arc across multiple epochs. This formulation of the requirements captures the progressive nature of a product's development process and lifetime; we refer to them as the product cycle in the remainder of the paper. A corresponding decision arc is found by optimization such that excess is minimized while reliability is maintained above a threshold. The decision arc can be traced to obtain a design alternative. In this manner, Monte Carlo simulation is used to generate multiple requirement arcs to obtain a set of solutions that balances robustness with flexibility by minimizing excess.

Our approach differs from the one in [17] in that we obtain set-based solutions by minimizing a cost function in terms of excess. Furthermore, categorical design variables are considered during the progressive upgrade of the design.

### 3.1 Relevant design metrics

The parameter vector $\mathbf{p} = [p_1, \ p_2, \ \cdots, \ p_n]^{\mathrm{T}} \in \mathbb{R}^n$, consists of $n$ parameters that may change [2]. In context of the bookshelf example, a design parameter would be the weight of the books. The feasibility criteria are formulated as constraints that the design must satisfy $\mathbf{t} - \mathbf{g}_f(\mathbf{p}) \leq 0$, where $\mathbf{t}$ is a vector of threshold values that the constraint function $\mathbf{g}_f(\mathbf{p})$ must exceed. For example, the safety factor of the book shelf for a given book must be greater than 2. Unlike requirements, feasibility constraints are fixed throughout the product cycle. Capability is defined as the set of possible values of a design parameter for which feasibility is maintained [2] (The set of books for which the safety factor is greater than 2):

$$C = \left\{ \mathbf{p} \in \mathbb{R}^n \mid \mathbf{t} - \mathbf{g}_f(\mathbf{p}) \leq 0 \right\}. \tag{1}$$

We represent requirements using a joint probability density function (PDF) $F_{\mathbf{X}}(\mathbf{p})$ [19, 27, 28, 29]. For example, the book shelf must support all books between 10 and 20 kg with a safety factor of at least 2. In practice such probability distributions can be constructed from previous knowledge regarding the uncertain parameters. For example, a sample of books can be weighed and their mean weight, lower, and upper bounds can be recorded to formulate a requirement. Knowing the capability of a design and the corresponding requirement joint PDF we can calculate reliability in terms of the probability that the design satisfies the requirement [30, 31]:

$$\mathbb{P}(\mathbf{p} \in C) = \frac{\int\limits_{C \cap R} F_{\mathbf{X}}(\mathbf{p}) d\mathbf{p}}{\int\limits_{R} F_{\mathbf{X}}(\mathbf{p}) d\mathbf{p}}. \tag{2}$$

$R$ in the denominator is the requirement set defined by the set of parameter values that yield significant probability density values from the joint PDF used.

The requirement set $R$ for a uniform PDF is given by

$$F_{\mathbf{X}}(\mathbf{p}) = \begin{cases} \dfrac{1}{\prod\limits_{j=1}^{n} |b_j - a_j|} & \text{for } \mathbf{a} \leq \mathbf{p} \leq \mathbf{b}, \\ 0 & \text{for } \mathbf{p} < \mathbf{a} \text{ or } \mathbf{p} > \mathbf{b} \end{cases}, \tag{3}$$

where $\mathbf{a}$ and $\mathbf{b}$ are the lower and upper bound vectors respectively. The requirement set $R$ comprises the values of $\mathbf{p}$ that lie within the bounds $\mathbf{a}$ and $\mathbf{b}$:

$$R = \left\{ \mathbf{p} \in \mathbb{R}^n \mid \mathbf{a} \leq \mathbf{p} \leq \mathbf{b} \right\}. \tag{4}$$

The Gaussian joint PDF is given by

$$F_{\mathbf{X}}(\mathbf{p}) = \frac{\exp\left(-\frac{1}{2}(\mathbf{p} - \mu)^{\mathrm{T}} \Sigma^{-1}(\mathbf{p} - \mu)\right)}{\sqrt{(2\pi)^n |\Sigma|}}, \tag{5}$$

where $\mu$ is the mean vector and $\Sigma$ is the covariance matrix. In this paper, we assume that parameters are uncorrelated. This results in a diagonal covariance matrix given by $\Sigma = \mathrm{diag}(\sigma)$, where $\sigma$ is the standard deviation vector. In the denominator of Equation (5), $|\Sigma| \equiv \det \Sigma \equiv \prod\limits_{j=1}^{n} \sigma_j$. The requirement set $R$ is defined as the values of $\mathbf{p}$ that result in a probability density level greater than that at the $3\sigma$ isocontour of a Gaussian $F_{\mathbf{X}}(\mathbf{p})$.

$$R = \left\{ \mathbf{p} \in \mathbb{R}^n \mid F_{\mathbf{X}}(\mathbf{p}) \geq F_{\mathbf{X}}(\mu + [3\sigma_1 \ 0 \ \cdots \ 0]^{\mathrm{T}}) \right\}. \tag{6}$$

This is because the probability that a random parameter value sampled from a Gaussian PDF lies outside the $3\sigma$ isocontour is small ($< 0.3\%$). Note that $F_{\mathbf{X}}(\mu + [3\sigma_1\ 0\ \cdots\ 0]^{\mathrm{T}}) \equiv F_{\mathbf{X}}(\mu + [0\ 3\sigma_2\ \cdots\ 0]^{\mathrm{T}}) \equiv F_{\mathbf{X}}(\mu + [0\ 0\ \cdots\ 3\sigma_n]^{\mathrm{T}})$ since they all lie on the $3\sigma$ isocontour.

We use Monte Carlo integration to approximate the integrals in Equation (2). Monte Carlo integration based on Latin hypercube (LH) sampling has the advantage of scaling well with dimensionality of the problem [32, 33], while importance sampling can be used in the case of a Gaussian PDF to enhance the accuracy of the approximation [28, 30, 34]. The Monte Carlo approximation is given by

$$\mathbb{P}(\mathbf{p} \in C) \approx \frac{\sum_{i=1}^{|C \cap R|} F_{\mathbf{X}}(\mathbf{p}_i)}{\sum_{i=1}^{|R|} F_{\mathbf{X}}(\mathbf{p}_i)}. \tag{7}$$

We use a two-dimensional parameter space shown in Figure 2 to illustrate the calculation of the reliability represented by $\mathbb{P}(\mathbf{p} \in C)$. Only the Monte Carlo samples that lie within the set $C$ (black dots) are evaluated by $F_{\mathbf{X}}(\mathbf{p})$ and summed to compute the numerator of Equation (7). All the Monte Carlo samples shown in Figure 2 (black and red dots) are evaluated by $F_{\mathbf{X}}(\mathbf{p})$ and summed to compute the denominator of Equation (7).

Buffer is defined in the parameter space as the portion of the capability of a design reserved for changes in requirements [2]. In other words, the buffer set is defined as the intersection of sets $C$ and $R$

$$B = \{\mathbf{p} \in \mathbb{R}^n \mid \mathbf{p} \in (C \cap R)\}. \tag{8}$$

The region given by intersection of the compliment of capability $C'$ and the requirement set $R$ is the opposite of buffer and endangers the design's ability to meet the requirements. This danger zone is defined as follows

$$D = \{\mathbf{p} \in \mathbb{R}^n \mid \mathbf{p} \in (C' \cap R)\}. \tag{9}$$

Excess is defined as the portion of the parameter space reserved for possible future changes in the requirements [2]. This is reflected by the set of parameter values that lie within the capability set $C$ but not within the requirement set $R$.

$$E = \{\mathbf{p} \in \mathbb{R}^n \mid \mathbf{p} \in (C \cap R')\}. \tag{10}$$

Note that $B \cup E = C$.

We are particularly interested in minimizing excess during the product redesign cycle. We estimate excess using the volume of the set $E$

$$V_E \approx \frac{1}{N} \sum_{i=1}^{N} H(\mathbf{p}_i), \text{ where } H(\mathbf{p}_i) = \begin{cases} 1 & \text{if } \mathbf{p}_i \in E \\ 0 & \text{otherwise} \end{cases}, \tag{11}$$

where $N$ is the number of samples from the parameter space used for the integration. We can use the reliability calculation and the volume of the requirement set $R$ to estimate the volume of the set $E$ indirectly. The volume of $R$ can be computed analytically for a uniform or Gaussian distribution using the corresponding hyper-rectangle or hyper-ellipsoid, respectively:

$$V_R = \begin{cases} \prod_{j=1}^{n} |b_j - a_j| & \text{if } F_{\mathbf{X}}(\mathbf{p}) \text{ is uniform} \\ \frac{\pi^2}{32} \prod_{j=1}^{n} |b_j - a_j| & \text{if } F_{\mathbf{X}}(\mathbf{p}) \text{ is Gaussian} \end{cases}. \tag{12}$$

We can then estimate the volume of set $C$ similarly:

$$V_C \approx \frac{1}{N} \sum_{i=1}^{N} H(\mathbf{p}_i), \text{ where } H(\mathbf{p}_i) = \begin{cases} 1 & \text{if } \mathbf{p}_i \in C \\ 0 & \text{otherwise} \end{cases}. \tag{13}$$

The reliability approximates the percentage of $R$ in $C$ and can be used as as proxy for the volume of $C \cap R$ such that $V_{C \cap R} \approx \mathbb{P}(\mathbf{p} \in C) \times V_R$. $V_E$ can now be approximated using

$$V_E \approx V_C - \mathbb{P}(\mathbf{p} \in C) \times V_R. \tag{14}$$

The sets $C, R, B, D$, and $E$ are shown in Figure 2 for a uniform and Gaussian requirement PDF. Having defined all the required design metrics, we can formulate an optimization problem to minimize excess subject to reliability constraints. We first set the context of the optimization problem in terms of an epoch-era analysis [22] to simulate changing requirements throughout the product cycle.

## 3.2 Epoch-era analysis for product redesign

We consider the redesign of component as time progresses through its development and lifecycle. At every epoch in the product cycle, the designer must make redesign decisions. The set of redesign choices is defined as the set of non-negative integers $\mathcal{D} = \{0, 1, 2, \cdots, q\}$. Chaining multiple choices together results in a design alternative defined as

$$\mathbf{D} = [D_1, D_2, \cdots, D_o] \tag{15}$$

with possible choices $D_d \in \mathcal{D}^o$, where $1 \leq o \leq q + 1$. The maximum number of redesign choices $q + 1$ dictates the maximum number of possible design alternative combinations where no choice is repeated twice. For example, consider a case where there are $q + 1 = 3$ redesign choices given by $\mathcal{D} = \{0, 1, 2\}$. If $o = 1$ then we have three possible design alternatives: $\mathbf{D} = [0]$, $\mathbf{D} = [1]$, and $\mathbf{D} = [2]$. For $o = 2$, 6 additional design alternatives can be obtained by permuting any 2 choices from $\mathcal{D}$. Similarly, another 6 design alternatives
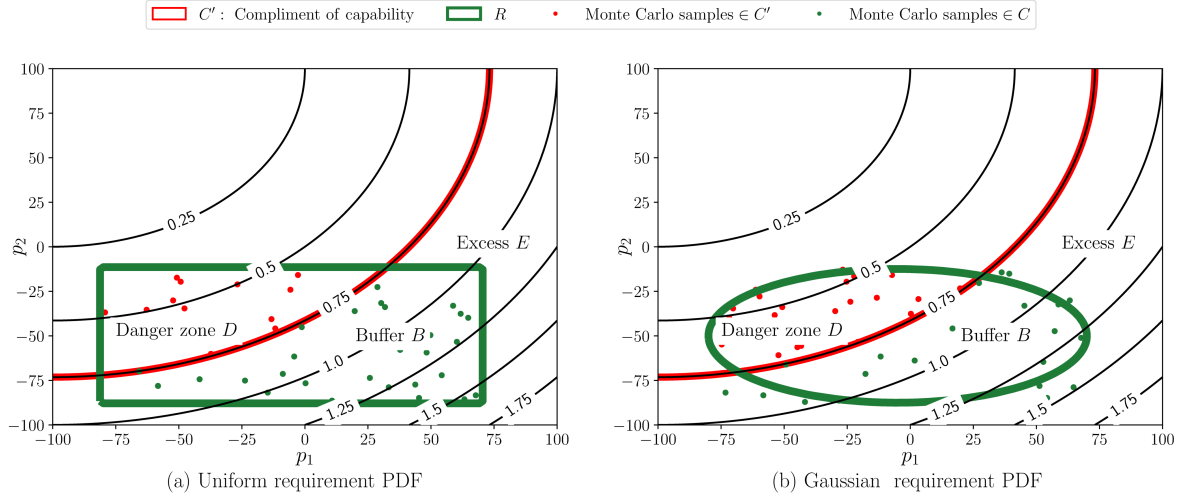
Fig. 2: Buffer and excess relative to a feasibility constraint $g_{f1}(\mathbf{p})$ in the two-dimensional parameter space for uniform (left) and Gaussian (right) PDFs

can be obtained for $o = 3$ by permutating all three choices in set $\mathcal{D}$. A total of 15 design alternatives can be obtained from $\mathcal{D} = \{0, 1, 2\}$.

These enumerations comprise a set of possible design alternatives given by $\Omega_D$. The cardinality of $\Omega_D$ for a different number of redesign choices $q + 1$ is given by

$$\Omega_D = \sum_{o=1}^{q+1} {}^{q+1}P_o, \tag{16}$$

where ${}^{q+1}P_o$ is the number of ways for obtaining an ordered subset of $o$ elements from a set of $q + 1$ elements.

We define a product cycle with $m$ number of epochs and $m$ number of corresponding decisions $S \in \mathcal{S}^m$, where $S_k$ is the decision at epoch $k$ and $\mathcal{S}$ is the set of possible decisions. In this paper, we consider discrete redesign choices only. A non-negative integer value from the set $\mathcal{S}$ implies a redesign choice. A value of $-1$ implies no redesign is performed at the current epoch. This means that $\mathcal{S} = \{-1, 0, 1, 2, \cdots, q\}$, where $q + 1$ is the number of available redesign choices.

The vector of all the decisions taken throughout the product cycle is referred to as the decision arc and is defined as

$$\mathbf{S} = [S_1, S_2, \cdots, S_m]. \tag{17}$$

The decision arc $\mathbf{S}$ has as many components as there are epochs. This is because a fixed number of decisions are made regarding redesign (including the choice to not redesign the TRS).

The set of possible decision arcs that can be generated from the set of possible decisions $\mathcal{S}$ may be restricted by constraints. A feasible decision arc cannot contain repeated choices. For example, the decision arc $\mathbf{S} = [0, -1, 0, -1, 1, 3]$ is infeasible since the choice 0 was

repeated twice. This constraint is specific to the application example in this paper because of the AM process used to effect the change. A design change cannot be retracted but choosing not to redesign the TRS ($S_n = -1$, $S_{n+1} = -1$) multiple times is viable. Furthermore, the first decision cannot be empty, i.e. $S_1 \neq -1$. This is because a decision arc must begin with some sort of design. These restrictions make computing the cardinality of the set of possible decision arcs $\Omega_S$ challenging. However, the cardinality of $\Omega_S$ is given by a finite positive integer similar to $\Omega_D$ in Equation (16).

A corresponding design alternative can be extracted from the decision arc by removing all negative elements from $\mathbf{S}$ to obtain $\mathbf{D} = [0, 2, 1, 3]$.

For each epoch $k$, a design alternative can be extracted by excluding values from $\mathbf{S}$ that are equal to $-1$. The vector $\mathbf{D}_k = [D_1, D_2, \cdots, D_o]$ represents this design alternative at epoch $k$ where the elements of $\mathbf{D}$ are non-negative integers and $o$ is the number of non-negative integers in $\mathbf{S}_k = [S_1, S_2, \cdots, S_k]$ up to the current epoch $k$. E.g., for a problem with $m = 6$ epochs and the decision arc

$$\mathbf{S} = [0, -1, 2, -1, 1, 3],$$

the following $m = 6$ design alternatives can be extracted

$$\text{epoch } k = 1 : \mathbf{D}_1 = [0]$$
$$\text{epoch } k = 2 : \mathbf{D}_2 = [0]$$
$$\text{epoch } k = 3 : \mathbf{D}_3 = [0, 2]$$
$$\text{epoch } k = 4 : \mathbf{D}_4 = [0, 2]$$
$$\text{epoch } k = 5 : \mathbf{D}_5 = [0, 2, 1]$$
$$\text{epoch } k = 6 : \mathbf{D}_6 = [0, 2, 1, 3].$$

It follows that a design alternative cannot feature repeated elements due to the uniqueness of the positive decision arc

6

elements. Each design alternative has a unique capability set $C_k$.

We now define the requirement arc as a vector of joint PDFs that has $m$ elements, where each element corresponds to a different epoch $k$ with a requirement joint PDF $F_{\mathbf{X}k}(\mathbf{p})$:

$$\mathbf{R} = [F_{\mathbf{X}1}(\mathbf{p}), \ F_{\mathbf{X}2}(\mathbf{p}), \ \cdots, \ F_{\mathbf{X}m}(\mathbf{p})]. \qquad (18)$$

The reliability at epoch $k$ (quantified by $\mathbb{P}_k(\mathbf{p} \in C_k)$) can be calculated from $C_k$ (derived from $\mathbf{D}_k$) and the requirement joint PDF $F_{\mathbf{X}k}(\mathbf{p})$:

$$\mathbf{P}(\mathbf{p} \in \mathbf{C}) = [\mathbb{P}_1(\mathbf{p} \in C_1), \ \mathbb{P}_2(\mathbf{p} \in C_2), \ \cdots, \ \mathbb{P}_m(\mathbf{p} \in C_m)], \qquad (19)$$

where $\mathbf{C}$ is the vector of capability sets $\mathbf{C} = [C_1, C_2, \cdots, C_m]$.

At each epoch, a reliability threshold $P_k$ is defined to yield a vector of reliability thresholds defined as

$$\mathbf{P}_{th} = [P_1, P_2, \cdots, P_m]. \qquad (20)$$

The volume of the excess set $V_{Ek}$ at epoch $k$ can be calculated from $C_k$ and the requirement joint PDF $F_{\mathbf{X}k}(\mathbf{p})$ using Equations (10) and (14). The cumulative excess for a given decision arc can be formulated as

$$E_c = \sum_{k=1}^{m} V_{Ek}. \qquad (21)$$

In addition to the decision arc $\mathbf{S}$, a fixed design concept $c_t \in \mathcal{C}$ is defined. The concept type $c_t$ is selected at the very beginning of the epoch-era analysis and does not change throughout epochs. The choice of $c_t$ dictates the list of redesign choices available for the remainder of the product cycle. $\mathcal{C}$ is the set of concept choices whose elements are all non-negative integers. This means that $\mathcal{C} = \{0, 1, 2, \cdots, r\}$, where $r + 1$ is the number of available concept choices.

Each concept type $C_t$ has a set of redesign options $\mathcal{D}_t$ with $q + 1$ redesign choices attached to it. Accordingly, each concept type $c_t$ will have a set of possible design alternatives $\Omega_{Dt}$ and a set of possible decision arcs $\Omega_{St}$. The combination of a concept and design alternative $\{c, \mathbf{D}\}$ will be referred to as a design alternative in this paper for conciseness. Similarly, the combination of a concept and a decision arc $\{c, \mathbf{S}\}$ will be referred to as a decision arc.

The cardinality of the set of possible design alternatives $\Omega_{cD}$ can be obtained by summing up the cardinalities of all sets $\Omega_{Dt}$ for a given set of concept choices $\mathcal{C}$:

$$\beta = |\Omega_{cD}| = \sum_{t=0}^{r} |\Omega_{Dt}|, \qquad (22)$$

where $|\Omega_{Dt}|$ can be obtained from Equation (16) given the number of redesign choices $q + 1$ for each concept. The set

of possible design alternatives represents the feasible design space, defined as

$$\Omega_{cD} = \left\{ \{c, \mathbf{D}\}_1, \{c, \mathbf{D}\}_2, \cdots, \{c, \mathbf{D}\}_\beta \right\}. \qquad (23)$$

We now formulate an optimization problem for choosing the optimal concept $c$ and decision arc $\mathbf{S}$ such that cumulative excess $E_c$ is minimized subject to reliability constraints:

$$\begin{aligned} \underset{\{c, \mathbf{S}\} \in \Omega_{cS}}{\text{minimize}} \quad & f(c, \mathbf{S}; \mathbf{R}) = E_c = \sum_{k=1}^{m} V_{Ek}(c, \mathbf{D}_k; F_{\mathbf{X}k}(\mathbf{p})) \\ \text{subject to} \quad & \mathbf{g}(c, \mathbf{S}; \mathbf{R}) = \mathbf{P}_{th} - \mathbf{P}(\mathbf{p} \in \mathbf{C}) \leq \mathbf{0}, \end{aligned} \qquad (24)$$

where $\Omega_{cS}$ denotes the set of all feasible decision arcs.

The problem in Equation (24) is solved using the mixed variable optimization variant of the mesh adaptive direct search (MADS) algorithm provided by the NOMAD software package [35]. This implementation of MADS allow users to specify categorical constraints via an extended poll subroutine and is called during the search step [36, 37].

The solutions of the problem given by Equation (24) depends on the requirement arc. Requirements are subject to change; therefore, we adopt a set-based design strategy to address such requirement changes.

### 3.3 Set-based design to mitigate changing requirements

Our set-based design strategy involves sampling requirement arcs $\mathbf{R}$ from the set of possible requirement arcs $\Omega_R = \{\mathbf{R}_1, \mathbf{R}_2 \cdots, \mathbf{R}_s\}$ with $s = |\Omega_R|$. A sample $\mathbf{R}_w$ involves populating the requirement arc with joint PDFs at each epoch $k$ by selecting a joint PDF from the set of possible joint PDFs $\mathcal{R} = \{F_{\mathbf{X}1}(\mathbf{p}), F_{\mathbf{X}2}(\mathbf{p}), \cdots, F_{\mathbf{X}v}(\mathbf{p})\}$, where $v$ is the number of joint PDF choices.

Populating the set $\mathcal{R}$ is based on the designer's experience and previous knowledge in requirements. E.g., if requirements are expected to become well-defined over time around a certain value in the parameter space, then a matrix of mean vectors $\mathbf{M} = [\mu_1, \mu_2, \cdots, \mu_e]^\mathrm{T}$ and a matrix of standard deviation vectors $\Sigma = [\sigma_1, \sigma_2, \cdots, \sigma_e]^\mathrm{T}$ can be obtained by using $e$ interpolation levels between the initial and final states for each type of joint PDF given by the set $\mathcal{T}$.

The set of possible requirement arcs $\Omega_R$ spans every possible combination of the joint PDFs (their type, mean, and standard deviation) and has a cardinality given by

$$\begin{aligned} v &= e \times e \times |\mathcal{T}| \ \text{and} \\ s &= |\Omega_R| = m^v, \ \text{respectively.} \end{aligned}$$

The first set-based solution is obtained by solving the optimization problem in Equation (24) for every requirement arc sample $\mathbf{R}_w$. The corresponding optimal design alternative $\mathbf{D}^*$ can be extracted from the optimal decision arc $\mathbf{S}^*$ to obtain the solution $\mathbf{x}^*(\mathbf{R}_w) = \{c^*, \mathbf{D}^*\}(\mathbf{R}_w)$. This is done in

7

order to compare the overdesign levels across different design alternatives rather than different decision arcs.

The set of parametric optimal design alternatives with respect to excess is defined as

$$S_E^* = \{\mathbf{x}^*(\mathbf{R}_1), \mathbf{x}^*(\mathbf{R}_2) \cdots, \mathbf{x}^*(\mathbf{R}_s)\}. \tag{25}$$

We track the number of times a specific design alternative $\{c, \mathbf{D}\}_\lambda$ appears as the solution to the parametric optimization problem in $S_E^*$ via a design optimality vector defined as

$$\mathbf{N}_E = \begin{bmatrix} n_{E1}, & n_{E2}, & \cdots, & n_{E\beta} \end{bmatrix}, \tag{26}$$

where $n_{E\lambda}$ is equal to the number of times design alternative $\{c, \mathbf{D}\}_\lambda \in \Omega_{cD}$ is repeated in $S_E^*$. The top $\alpha$ design alternatives with the largest $n_{E\lambda}$ values are selected as the set-based solution representing the best performing design alternatives in terms of minimizing overdesign:

$$S_E = \{\{c, \mathbf{D}\}_{E1}, \{c, \mathbf{D}\}_{E2} \cdots, \{c, \mathbf{D}\}_{E\alpha}\}. \tag{27}$$

The rationale for selecting $\alpha$ will be described in the context of the application example presented in this paper.

The pseudo-algorithm in Algorithm 1 summarizes the above described method for obtaining the sets of optimal design alternatives with respect to excess.

The second set-based solution is the robust design set. We define robustness of a design alternative by the number of design alternatives satisfied from the set $\Omega_R$. We evaluate the feasibility of each design alternative $\{c, \mathbf{D}\}_\lambda$ sampled from the set of possible design alternatives in Equation (23) with respect to every requirement arc $\mathbf{R}_w$ in $\Omega_R$.

We generate all the possible decision arcs for a given design alternative $\{c, \mathbf{D}\}_\lambda$ by randomly inserting the $-1$ decisions into the design alternative vector until it has the same number of elements as the number of epochs $m$. We show this using an example. Consider the design alternative $\{c = 1, \mathbf{D} = [2, 0, 1]\}$. The possible decision arcs are

$$\{c = 1, \mathbf{S} = [2, -1, -1, -1, 0, 1]\}$$
$$\{c = 1, \mathbf{S} = [2, -1, -1, 0, -1, 1]\}$$
$$\{c = 1, \mathbf{S} = [2, -1, -1, 0, 1, -1]\}$$
$$\{c = 1, \mathbf{S} = [2, -1, 0, -1, 1, -1]\}$$
$$\{c = 1, \mathbf{S} = [2, -1, 0, 1, -1, -1]\}$$
$$\{c = 1, \mathbf{S} = [2, 0, -1, 1, -1, -1]\}$$
$$\{c = 1, \mathbf{S} = [2, 0, 1, -1, -1, -1]\},$$

yielding the set of decision arcs with $\zeta = 7$ elements

$$S_{cD} = \{\{c, \mathbf{S}\}_1, \{c, \mathbf{S}\}_2 \cdots, \{c, \mathbf{S}\}_7\}. \tag{28}$$

Feasibility in terms of reliability is checked for every possible decision arc $\{c, \mathbf{S}\}_\gamma$ for a given $\{c, \mathbf{D}\}_\lambda$ and requirement arc $\mathbf{R}_w$ using $\mathbf{g}(c_\gamma, \mathbf{S}_\gamma; \mathbf{R}_w) = \mathbf{P}_{th} - \mathbf{P}(\mathbf{p} \in \mathbf{C}) \leq \mathbf{0}$. If any of the decision arcs in set $S_{cD}$ satisfy all the reliability constraints then the corresponding design alternative $\{c, \mathbf{D}\}_\lambda$ is considered feasible. We track the number of requirement arcs satisfied by design alternative $\{c, \mathbf{D}\}_\lambda$ through a robustness vector defined as

$$\mathbf{N}_R = \begin{bmatrix} n_{R1}, & n_{R2}, & \cdots, & n_{R\beta} \end{bmatrix}, \tag{29}$$

where $n_{R\lambda}$ is equal to the number of requirement arcs $\mathbf{R}_w \in \Omega_R$ satisfied by design alternative $\{c, \mathbf{D}\}_\lambda \in \Omega_{cD}$. The top $\alpha$ design alternatives with the largest $n_{R\lambda}$ values are considered as the robust design set:

$$S_R = \{\{c, \mathbf{D}\}_{R1}, \{c, \mathbf{D}\}_{R2} \cdots, \{c, \mathbf{D}\}_{R\alpha}\}. \tag{30}$$

The final set-based solution is the flexible design set. All possible design alternatives in set $\Omega_{cD}$ are ranked in terms of filtered outdegree, defined as the number of possible design alternatives that can be obtained from the current design alternative by adding exactly one redesign choice that is not an element of the current design alternative. The filtered part is determined by which design changes are allowed when going from one design "state" to another. For example, the possible designs that can be obtained from $\mathbf{D} = [0, 1]$ are $[0, 1, 2]$ or $[0, 1, 3]$ (the outdegree) if only three deposits are considered. In this way other designs such as $[2, 1, 0], [1, 0, 2], \cdots$ etc. are filtered out when considering the flexibility of design alternative $\mathbf{D} = [0, 1]$. The filtered outdegree for a design alternative $\{c, \mathbf{D}\}_\lambda$ having $o$ elements and $q + 1$ redesign choices is equal to

$$O_{F_\lambda} = q - o. \tag{31}$$

The top $\alpha$ design alternatives in terms of filtered outdegree are considered as the flexible design set:

$$S_F = \{\{c, \mathbf{D}\}_{F1}, \{c, \mathbf{D}\}_{F2} \cdots, \{c, \mathbf{D}\}_{F\alpha}\}. \tag{32}$$

The pseudo-algorithm in Algorithm 2 summarizes the above described method for obtaining the sets of robust and flexible design alternatives.

We will now use a tradespace to visualize and compare these solution sets.

### 3.4 Tradespace exploration for comparing solution sets

A tradespace can be constructed by plotting the volume of the capability set $V_c$, against the weight of each design alternative. The volume of capability set is chosen as the utility since it is independent of the requirement joint PDF. This allows for a fair comparison between different design alternatives. The design alternatives in sets $S_E, S_R$, and $S_F$ are also

---
**Algorithm 1:** Pseudo-algorithm for obtaining the set of optimal design alternatives $S_E$
---
**Input:** Set of possible requirement arcs $\Omega_R$, Set of possible design alternatives $\Omega_{cD}$
**Output:** $S_E$

1   Initialize design optimality vector $\mathbf{N}_E = \left[n_{E1}, n_{E2}, \cdots, n_{E\beta}\right] = \mathbf{0}$
2   **for** $w = 1, 2, ..., s$ **do**
3     Solve the parametric optimization problem in Equation (24) to obtain optimal decision arc
      $\mathbf{x}_S^*(\mathbf{R}_w) = \{c^*, \mathbf{S}^*\}(\mathbf{R}_w)$
4     Reduce optimal decision arc to optimal design alternative by eliminating $-1$ components of $\mathbf{S}^*$ to obtain
      $\mathbf{x}^*(\mathbf{R}_w) = \{c^*, \mathbf{D}^*\}(\mathbf{R}_w)$
5     Augment $S_E^* \leftarrow S_E^* \cup \{\mathbf{x}^*(\mathbf{R}_w)\}$
6     Find $\lambda$ corresponding to $\{c^*, \mathbf{D}^*\}$
7     Award design alternative $n_{E\lambda} \leftarrow n_{E\lambda} + 1$
8   Sort design optimality vector $\mathbf{N}_E$ in descending order
9   Select top $\alpha$ design alternatives with largest values $n_{E\lambda}$ to obtain set of optimal designs
    $S_E = \{\{c, \mathbf{D}\}_{E1}, \{c, \mathbf{D}\}_{E2} \cdots, \{c, \mathbf{D}\}_{E\alpha}\}$

---
**Algorithm 2:** Pseudo-algorithm for obtaining the sets of robust $S_R$ and flexible $S_F$ design alternatives
---
**Input:** Set of possible requirement arcs $\Omega_R$, Set of possible design alternatives $\Omega_{cD}$
**Output:** $S_R, S_F$

1   Initialize design robustness vector $\mathbf{N}_R = \left[n_{R1}, n_{R2}, \cdots, n_{R\beta}\right] = \mathbf{0}$
2   **for** $\lambda = 1, 2, ..., \beta$ **do**
3     Enumerate possible decision arcs from $\{c, \mathbf{D}\}_\lambda$ to obtain the set $S_{cD} = \left\{\{c, \mathbf{S}\}_1, \{c, \mathbf{S}\}_2 \cdots, \{c, \mathbf{S}\}_\zeta\right\}$
4     **for** $w = 1, 2, ..., s$ **do**
5       **for** $\gamma = 1, 2, ..., \zeta$ **do**
6         **if** $\mathbf{g}(c_\gamma, \mathbf{S}_\gamma; \mathbf{R}_w) \leq \mathbf{0}$ **then**
7           Award design alternative $n_{R\lambda} \leftarrow n_{R\lambda} + 1$
8           **break**
9     Compute filtered outdegree for $\{c, \mathbf{D}\}_\lambda$ using $O_{F_\lambda} = q - o$
10    Augment design flexibility vector $\mathbf{N}_F \leftarrow \mathbf{N}_F \cup \{O_{F_\lambda}\}$
11   Sort design robustness vector $\mathbf{N}_R$ in descending order
12   Select top $\alpha$ design alternatives with largest values $n_{R\lambda}$ to obtain set of robust design alternatives
    $S_R = \{\{c, \mathbf{D}\}_{R1}, \{c, \mathbf{D}\}_{R2} \cdots, \{c, \mathbf{D}\}_{R\alpha}\}$
13   Sort design flexibility vector $\mathbf{N}_F$ in descending order
14   Select top $\alpha$ design alternatives with largest values $O_{F_\lambda}$ to obtain set of flexible design alternatives
    $S_F = \{\{c, \mathbf{D}\}_{F1}, \{c, \mathbf{D}\}_{F2} \cdots, \{c, \mathbf{D}\}_{F\alpha}\}$

---

projected on the same tradespace to compare their relative position and size. The Pareto front for such a tradespace can be approximated by solving the bi-objective problem

$$\underset{\{c, \mathbf{D}\} \in \Omega_{cD}}{\text{minimize}} \quad \left[-V_c(c, \mathbf{D}) \quad W(c, \mathbf{D})\right] \tag{33}$$

The positioning of sets $S_E, S_R$, and $S_F$ relative to the Pareto set obtained by solving the problem in Equation (33) provides a measure for the dominance of each design set.

## 4   Application

We demonstrate the importance of minimizing excess in aerospace structural component design by applying our method to the design of a turbine rear structure (TRS). The TRS is a structural component located after a jet engine's turbines to direct exhaust gases. The TRS shown in Figure 3a is subject to thermal loads due to temperature gradients experienced during operation. The temperature profile of a TRS during operation is shown in Figure 3b. These temperature loads are specified by the OEM engine architect to the TRS component supplier in the form of changing parameters. The TRS is remanufactured using AM to increase the stiffness of the outer casing in response to changing requirements (temperature loads). The TRS can undergo multiple redesigns as given by a decision arc during its product cycle. We will now describe the available stiffener designs.

### 4.1   Stiffener deposition on TRS outer casing

Stiffeners deposited on the outer casing of the TRS involve the application of heat to the outer casing (the sub-

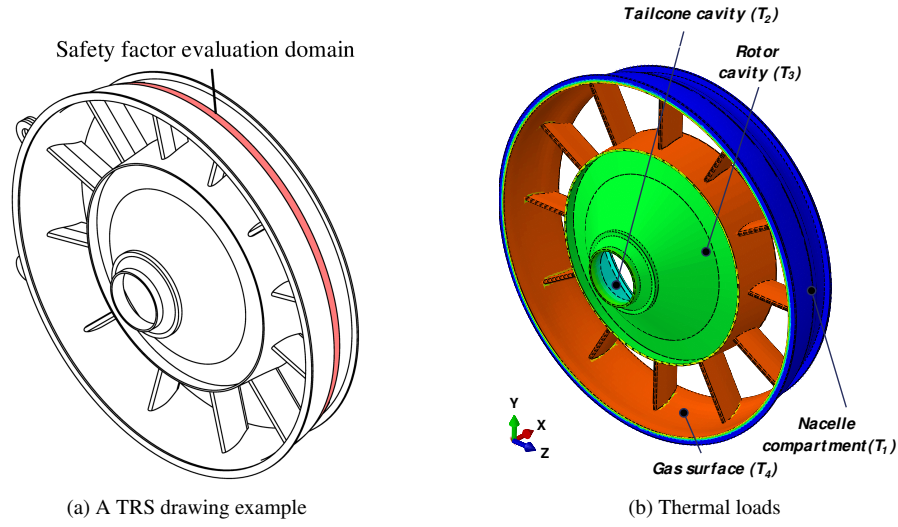(a) A TRS drawing example      (b) Thermal loads

Fig. 3: TRS remanufacturing example

strate) to deposit material on its surface. This causes residual distortion that persists after the removal of the heat source and affects the structural performance when loads are applied during operation. The residual stresses experienced by the TRS due to the deposition of a stiffener are quantified using previous results and analyses [38].

There are several stiffener geometries available to the designer of the TRS given by the set of possible design alternatives $\Omega_{cD}$. We draw inspiration from commonly used standard stiffener designs to generate concepts and design choices [39]. The design space consists of three possible deposition concepts $\mathcal{C} = \{0,1,2\}$. We illustrate these concepts and their respective design choices in Figure 4.

We compute the cardinality of the set $\Omega_{cD}$ using Equation (16), Equation (22) and the maximum of number of redesign choices obtained from Figure 4. Calculation of the cardinality is given by the following:

$$\text{concept } c_0 : \ |\Omega_{D0}| = 15$$
$$\text{concept } c_1 : \ |\Omega_{D1}| = 325$$
$$\text{concept } c_2 : \ |\Omega_{D2}| = 64$$
$$\beta = |\Omega_{cD}| = 15 + 325 + 64 = 404.$$

We now describe the analysis steps for obtaining the capability of a given stiffener design alternative as a function of the thermal temperature loads.

### 4.2 Loadcase description

The changing temperature loads in Figure 3b are used to specify the vector of changing parameters $\mathbf{p} = [T_1, T_2, T_3, T_4]^T$. We constrain our study to a parameter space defined by $\mathbf{p} \in \{\mathbf{p} : \mathbf{p}_{\text{nominal}} - \mathbf{p}_{\text{deviation}} \le \mathbf{p} \le \mathbf{p}_{\text{nominal}} + \mathbf{p}_{\text{deviation}}\}$, where $\mathbf{p}_{\text{nominal}} = [350, 425, 410, 580]^T$ and $\mathbf{p}_{\text{deviation}} = [100, 100, 100, 100]^T$.
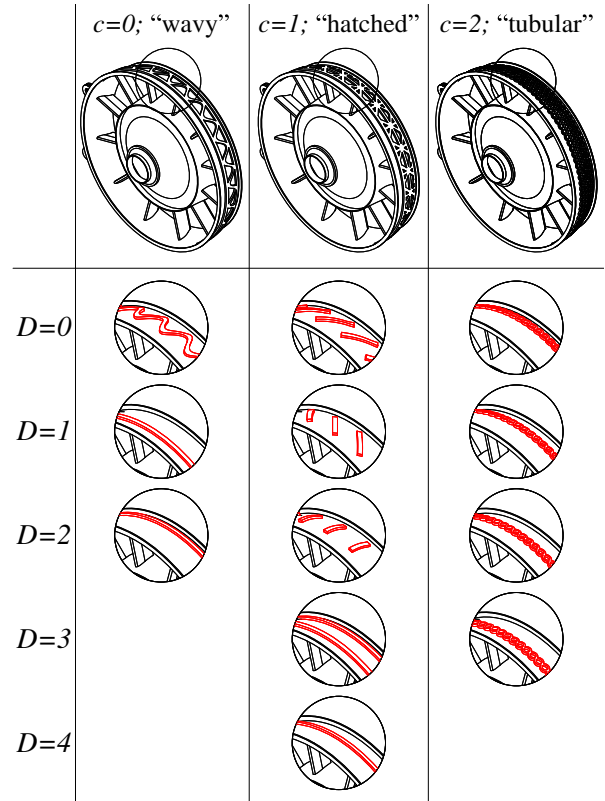


Fig. 4: Illustration of possible concepts and redesign choices for TRS stiffener

The thermal load case is cycled and is used to compute the expected fatigue life of the TRS using low-cycle fatigue calculations that were described in previous work [38]. The result of the the low-cycle fatigure analysis is a safety factor ($n_{\text{safety}}$) against low-cycle fatigue failure or yielding, whichever occurs first. The TRS design is constrained by a minimum safety factor equal to 2.8.

The structural analysis is performed using a finite element (FE) simulation model which is computationally expensive. As a result, for every design alternative in $\Omega_{cD}$, we build a surrogate model for computing $n_{\text{safety}}(\mathbf{p})$. The surrogate is built using data obtained from the simulation model for 25 Latin hypercube samples of the parameter space for every design in $\Omega_{cD}$. This resulted in $25 \times 404 = 10100$ samples for the surrogate. For this particular problem, the sampling was sufficient to capture the effect of increasing the internal temperature loads ($T_2$, $T_3$, and $T_4$) on decreasing $n_{\text{safety}}$ due to the expansion of the outercasing of the TRS. We use an open source surrogate model library to build and optimize the hyperparameters of an ensemble of surrogates [40].

Mathematically, we formulate the constraint on the safety factor as

$$t_1 - \hat{g}_{f1}(\mathbf{p}) \leq 0. \tag{34}$$

We visualize this constraint in the 4-dimensional parameter space for a few example design alternatives in Section 5.1.

### 4.3  Loadcase requirements

Having defined the 4-dimensional parameter space, we now define the joint PDFs and the corresponding requirement arcs that can be constructed from them. While we consider only two types ($\mathcal{T} = \{\text{uniform}, \text{Gaussian}\}$), any distribution can be used in our method.

All design metrics and requirements are scaled between 0 and 1. This helps when making comparisons between different design alternatives in terms of hypervolume of sets with 0 being the minimum possible hypervolume and 1 being the maximum possible hypervolume.

We use $e = 5$ interpolation levels to obtain $\mathbf{M}$ and $\Sigma$. The initial mean and standard deviation vectors are $\mu_1 = [0.15, 0.80, 0.80, 0.85]^{\text{T}}$ and $\sigma_1 = [0.1875, 0.125, 0.125, 0.1875]^{\text{T}}$, respectively. The final mean and standard deviation vectors are $\mu_5 = [0.85, 0.20, 0.20, 0.15]^{\text{T}}$ and $\sigma_5 = [0.375, 0.250, 0.250, 0.375]^{\text{T}}$, respectively. As a result, the matrix of interpolated mean and standard deviation vectors is

$$\mathbf{M} = \begin{bmatrix} \mu_1^{\text{T}} \\ \mu_2^{\text{T}} \\ \mu_3^{\text{T}} \\ \mu_4^{\text{T}} \\ \mu_5^{\text{T}} \end{bmatrix} = \begin{bmatrix} 0.15 & 0.80 & 0.80 & 0.85 \\ 0.325 & 0.65 & 0.65 & 0.675 \\ 0.5 & 0.5 & 0.5 & 0.5 \\ 0.675 & 0.35 & 0.35 & 0.325 \\ 0.85 & 0.20 & 0.20 & 0.15 \end{bmatrix}$$

and

$$\Sigma = \begin{bmatrix} \sigma_1^{\text{T}} \\ \sigma_2^{\text{T}} \\ \sigma_3^{\text{T}} \\ \sigma_4^{\text{T}} \\ \sigma_5^{\text{T}} \end{bmatrix} = \begin{bmatrix} 0.1875 & 0.125 & 0.125 & 0.1875 \\ 0.234375 & 0.15625 & 0.15625 & 0.234375 \\ 0.28125 & 0.1875 & 0.1875 & 0.28125 \\ 0.328125 & 0.21875 & 0.21875 & 0.328125 \\ 0.375 & 0.250 & 0.250 & 0.375 \end{bmatrix},$$

respectively.

We consider a remanufacturing design problem with $m = 6$ epochs. The number of choices $v$ for $\mathcal{R} = \{F_{\mathbf{X}1}(\mathbf{p}), F_{\mathbf{X}2}(\mathbf{p}), \cdots, F_{\mathbf{X}v}(\mathbf{p})\}$ and the cardinality $s$ for $\Omega_R$ are

$$v = e \times e \times |\mathcal{T}| = 5 \times 5 \times 2 = 50 \text{ and}$$

$$s = |\Omega_R| = m^v = 6^{50}, \text{ respectively.}$$

Only the first few elements of $\Omega_R$ will be used during the set-based design analysis and $s$ will be capped at $10^5$ samples. This is because the set-based solutions stabilize and do not change after sampling $4 \times 10^4$ requirement arc samples.

While we chose the following reliability threshold vector for this example

$$\mathbf{P}_{th} = [0.01, 0.1, 0.3, 0.3, 0.8, 0.9]^{\text{T}},$$

a design engineer can test and react to different lifecycle scenarios by adjusting the reliability threshold. In this application, the reliability is ramped up further down the design process to allow room for flexibility in the early conceptual stage but adds more restrictions on reliability as the project approaches completion. By contrast, the reliability threshold would be held constant as per industry standards to ensure safe operation when considering a design that is in operation.

## 5  Results and discussion

We initiate the solution of the remanufacturing design problem by obtaining the capability set for every design alternative in the set $\Omega_{cD}$. We begin by investigating a few selected design alternatives from $\Omega_{cD}$. We then solve a single optimization problem to minimize excess for a given requirement arc from the set $\Omega_R$. We then present the set-based results for the problem using a tradespace.

### 5.1  Example for calculating the design properties of a given design alternative

We use two design alternatives from the set $\Omega_{cD}$ to visualize feasible space, capability and reliability in two-dimensional projections of the four-dimensional parameter space in Figure 5.

We can observe that the addition of one more deposit to the design alternative $\{c = 1, \mathbf{D} = [1, 2, 4]\}$ increases its performance in terms of capability and reliability (given

11

by the larger capability set $C$ and its intersection with the requirement set $R$). By comparing Figures 5a ($\{c=1, \mathbf{D}=[1,2,4]\}$) and 5b ($\{c=1, \mathbf{D}=[1,2,4,0]\}$), it can be seen that the size of $C \cap R$ (given by the square hatched area) which represents reliability is larger for $\{c=1, \mathbf{D}=[1,2,4,0]\}$. However, this comes at the cost of an additional 4.6 kg of weight and reduced filtered outdegree. Figure 5b shows that $\{c=1, \mathbf{D}=[1,2,4,0]\}$ has an additional excess (given by the unhatched area) of 0.327 for a uniform PDF when compared to $\{c=1, \mathbf{D}=[1,2,4]\}$. Figure 5 shows the tradeoff between reliability and excess by examining their areas for two design alternatives. The choice of design alternative for a given requirement arc is driven by the need to maintain reliability while minimizing excess. We will apply epoch-era analysis and numerical optimization to solve related design decision problems.

## 5.2 Optimization with respect to a requirement arc

We solve the problem given by Equation (24) using a mixed variable programming version of MADS [35]. The requirement arc $\mathbf{R}_w$ used for this problem is given in Table 1.

Table 1: Requirement arc $\mathbf{R}_w$

| PDF Index $(F_{\mathbf{X}} \in \mathcal{R})$ | $F_{\mathbf{X}36}$ | $F_{\mathbf{X}50}$ | $F_{\mathbf{X}1}$ | $F_{\mathbf{X}46}$ | $F_{\mathbf{X}13}$ | $F_{\mathbf{X}31}$ |
|---|---|---|---|---|---|---|
| mean vector ($\mu$) | $\begin{bmatrix} 0.5 \\ 0.5 \\ 0.5 \\ 0.5 \end{bmatrix}$ | $\begin{bmatrix} 0.85 \\ 0.2 \\ 0.2 \\ 0.15 \end{bmatrix}$ | $\begin{bmatrix} 0.15 \\ 0.8 \\ 0.8 \\ 0.85 \end{bmatrix}$ | $\begin{bmatrix} 0.85 \\ 0.2 \\ 0.2 \\ 0.15 \end{bmatrix}$ | $\begin{bmatrix} 0.5 \\ 0.5 \\ 0.5 \\ 0.5 \end{bmatrix}$ | $\begin{bmatrix} 0.325 \\ 0.65 \\ 0.65 \\ 0.675 \end{bmatrix}$ |
| SD* vector ($\sigma$) | $\begin{bmatrix} 0.1875 \\ 0.125 \\ 0.125 \\ 0.1875 \end{bmatrix}$ | $\begin{bmatrix} 0.375 \\ 0.25 \\ 0.25 \\ 0.375 \end{bmatrix}$ | $\begin{bmatrix} 0.1875 \\ 0.125 \\ 0.125 \\ 0.375 \end{bmatrix}$ | $\begin{bmatrix} 0.1875 \\ 0.125 \\ 0.125 \\ 0.1875 \end{bmatrix}$ | $\begin{bmatrix} 0.28125 \\ 0.1875 \\ 0.1875 \\ 0.28125 \end{bmatrix}$ | $\begin{bmatrix} 0.1875 \\ 0.125 \\ 0.125 \\ 0.1875 \end{bmatrix}$ |
| type ($t$) | Gaussian | Gaussian | uniform | Gaussian | uniform | "Gaussian" |

*SD: standard deviation

We plot the results from various decision arcs across epochs in Figure 6. The first decision arc, $\{c=1, \mathbf{S}=[2,1,-1,-1,0,-1]\}$ (shown in red) does not satisfy the reliability constraint as shown in Figure 6a. This is because at epoch $k=3$ the reliability of the corresponding design alternative $\{c=1, \mathbf{D}=[2,1]\}$ is almost 0. No redesign occurred at epoch $k=3$ when it was needed to increase the reliability of the design alternative above the threshold.

We investigate another decision arc $\{c=1, \mathbf{S}=[4,1,0,2,-1,3]\}$ (shown in green) that achieves very high reliability throughout all epochs. However, this comes at the cost of increased cumulative excess (green shaded area in Figure 6b) relative to that of the first decision arc (red shaded area).

We solve the optimization problem given by Equation (24) to get the third decision arc $\{c=1, \mathbf{S}=[4,1,0,2,-1,3]\}$ (shown in blue) which is optimal in terms of minimizing excess. This decision arc has lower reliability relative to the second decision arc

(shown in green) but lower cumulative excess and therefore less overdesign. We provide the values of the objective function and reliability constraints for all three decision arcs in Table 2.

Table 2: Results obtained for example decision arcs given a requirement arc $\mathbf{R}_w$

| Decision arc $\{c, \mathbf{S}\}$ | Objective value $f(c, \mathbf{S}; \mathbf{R})$ | Reliability constraints $\mathbf{g}(c, \mathbf{S}; \mathbf{R})$ | Design alternative $\{c, \mathbf{D}\}$ |
|---|---|---|---|
| $\{c=1,$ $\mathbf{S}=[2,1,-1,-1,0,-1]\}$ | 3.91 | $\begin{bmatrix} -0.063 \\ -0.9 \\ 0.3 \\ -0.7 \\ -0.2 \\ -0.1 \end{bmatrix}$ | $\{c=1,$ $\mathbf{D}=[2,1,0]\}$ |
| $\{c=1,$ $\mathbf{S}=[4,1,0,2,-1,3]\}$ | 5.16 | $\begin{bmatrix} -0.94 \\ -0.9 \\ -0.70 \\ -0.7 \\ -0.20 \\ -0.1 \end{bmatrix}$ | $\{c=1,$ $\mathbf{D}=[4,1,0,2,3]\}$ |
| $\{c=1,$ $\mathbf{S}=[2,1,0,4,-1,3]\}$ | 4.58 | $\begin{bmatrix} -0.063 \\ -0.9 \\ -0.20 \\ -0.7 \\ -0.17 \\ -0.1 \end{bmatrix}$ | $\{c=1,$ $\mathbf{D}=[2,1,0,4,3]\}$ |

Finally, the example in this section shows that the order of redesign steps can have a significant impact on the reliability and level of overdesign throughout epochs. The second and third decision arcs contain the same redesign choices but in different order. Choosing the right order of redesign operations is important when considering multiple epochs.

## 5.3 Set-based design and tradespace exploration

We solve an optimization problem similar to the one in Section 5.2 for every requirement arc in $\Omega_R$ to obtain the set of parametric optimal design alternatives when optimizing for cumulative excess ($S_E^*$). For each design alternative in $\Omega_{CD}$, we plot the frequency of observations in $S_E^*$ normalized by the cardinality $\beta$ of set $\Omega_R$ to obtain the histogram shown in Figure 7. We evaluated the flexibility and robustness of each design alternative in $\Omega_{cD}$ using the method in Algorithm 2.

We select the top $\alpha = 10$ design alternatives in Figure 7 as our set of optimal design alternatives $S_E$. In practice, $\alpha$ is constrained by the designers' ability to concurrently develop and analyze the selected set of design alternatives. For example, development time and cost may limit the designers to a maximum of 10 designs that can be concurrently developed at any given time during development. Furthermore, the 10th design alternative in $S_E$ given by $\lambda = 278$ is representative of the lower ranking design alternatives since they all have comparable frequencies. A similar rationale is used for obtaining the set of robust design alternatives $S_R$. Only

(a) $\{c = 1, \mathbf{D} = [1, 2, 4]\}$



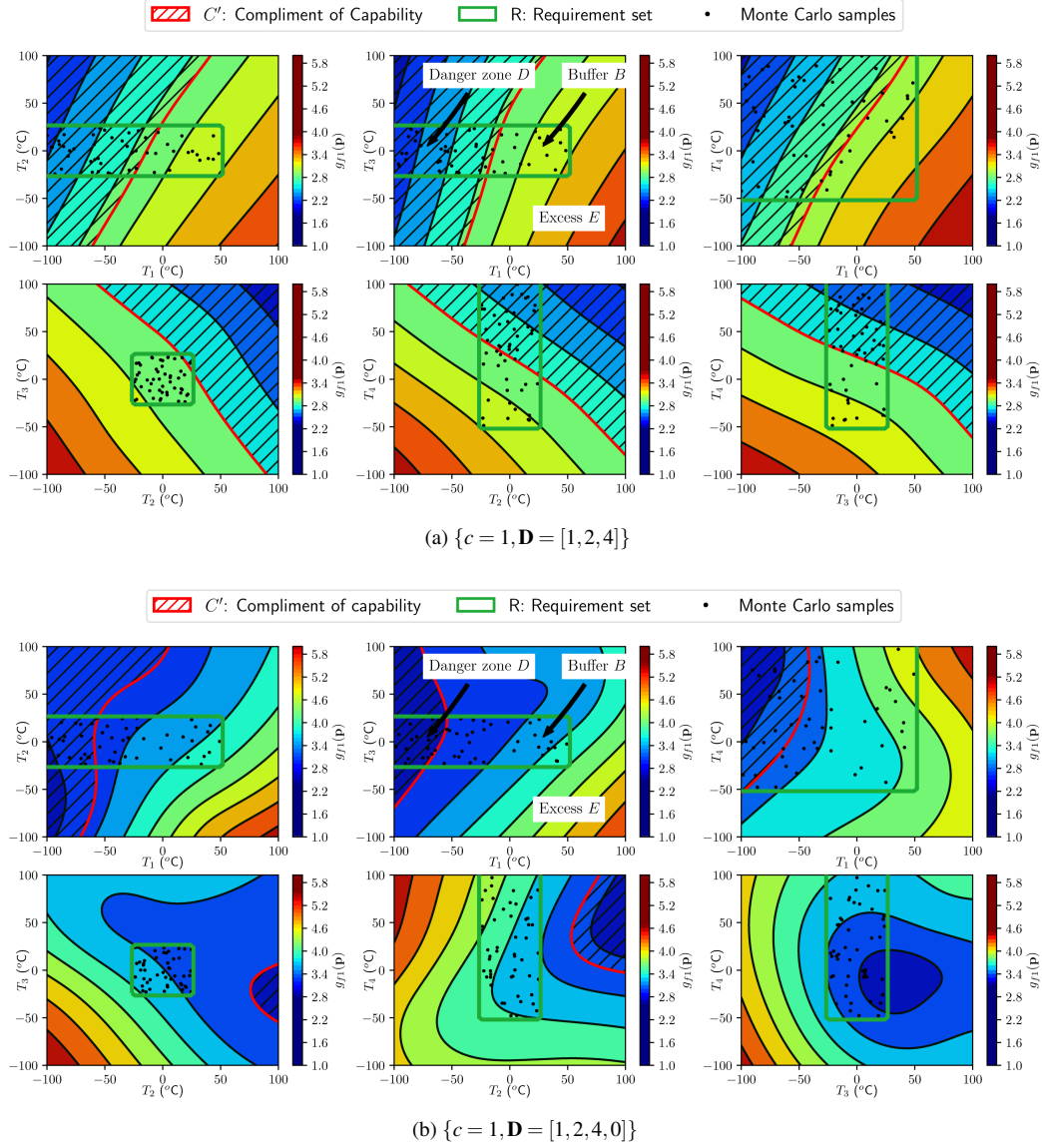(b) $\{c = 1, \mathbf{D} = [1, 2, 4, 0]\}$

Fig. 5: Two-dimensional projections of the four-dimensional parameter space

$\alpha = 5$ design alternatives are used to construct the flexible set-based solution $S_F$ since we focus on those designs with maximum possible filtered outdegree $O_F = 4$.

The sets $S_E$, $S_R$, and $S_F$ are visualized on a tradespace. This tradespace is described by a utility (given by the volume of the capability set $V_c$) and cost (given by the weight $W$) and is shown in Figure 8. The Pareto front for the tradespace is obtained by solving the problem in Equation (33).

From the tradespace, we can draw several insights. The flexible set-based solution minimizes cost but also minimizes utility. In contrast, the robust design set maximizes utility but also maximizes the cost. The set-based solutions obtained by optimization balances utility with cost. We quantify the size of the set-based solutions by their convex hulls. Convex hulls are used to calculate three metrics: the area spanned by the set, location of the set given by its centroid and proximity to the Pareto front given by the distance from the centroid to the nearest Pareto point [41]. We report these convex hull metrics in Table 3.

We can see that the set of optimal design alternatives with respect to cumulative excess $S_E$ occupies 10.4% which is comparable to that occupied by the set of flexible design alternatives $S_F$ and greater than that occupied by the set of robust design alternatives $S_R$. The set of optimal design alternatives $S_E$ is close to the Pareto front, since it aims to balance robustness with flexibility which are indirectly related to capability and weight.

We aim to analyze the top 6 designs in set $S_E$ in Figure 7 by examining the geometry of the deposits that belong to these designs in Figure 9.

Figure 9 shows that the top 6 designs in $S_E$ share the same concept $c = 1$. The top two designs ($\lambda = 82$ and $\lambda = 86$) share the first two deposit choices $D_1 = 1$ and $D_2 = 0$. The runner-up design ($\lambda = 86$) adds two additional deposits to the top ranked design ($\lambda = 82$). The addition of two more deposits to the top ranked design reduced the capability $V_c$.
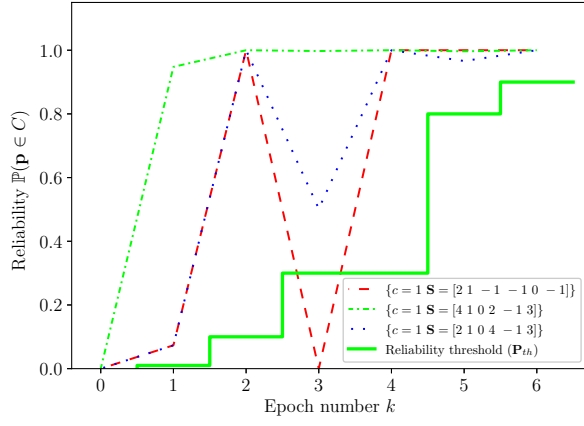
(a) Reliability
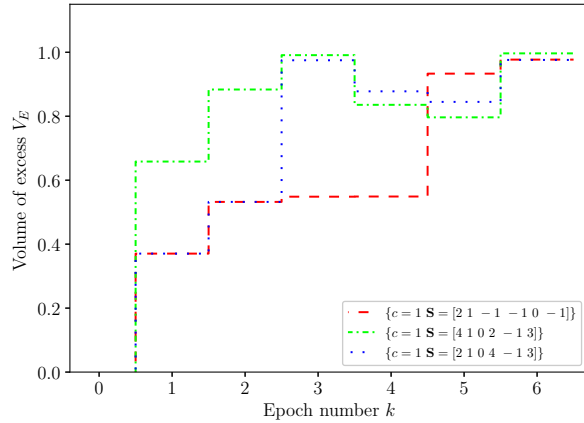


(b) Volume of excess set

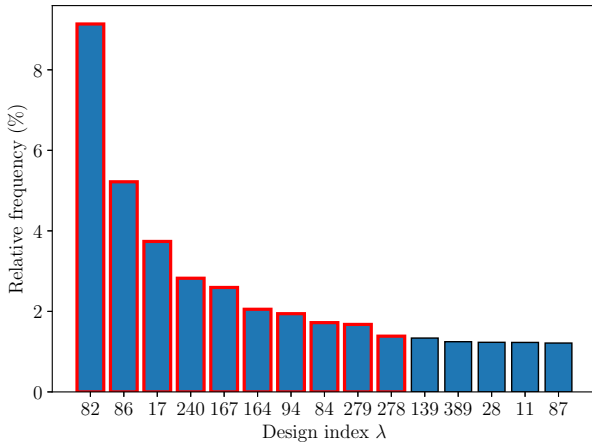Fig. 6: Visualization of decision arcs



Fig. 7: Distribution of optimal design alternatives in set-based solutions

This is because of the overstiffening of the TRS outer casing by the addition of more stiffeners. Designs $\lambda = 17$ and $\lambda = 82$ have the same deposits, but are ranked differently due to the difference in thermomechanical effect of depositing $D_1 = 0$ first instead of $D_1 = 1$.
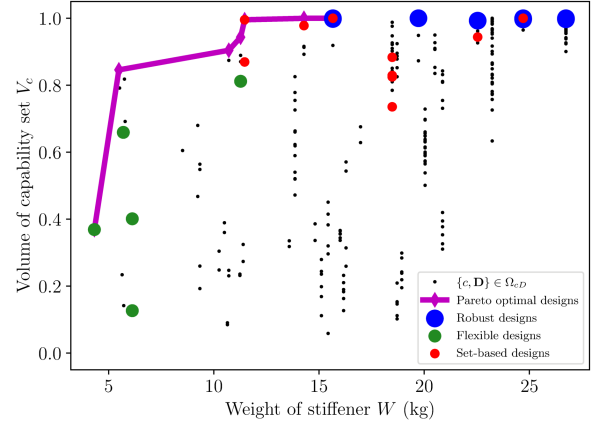


Fig. 8: Tradespace of set-based design alternatives

The tools developed in this paper can help designers make informed decisions about the sequence of redesign choices during a product cycle. These insights are particularly useful for determining the first redesign choice when uncertainty and the number of possible choices are high.

## 6  Discussion

The scope of this study focuses on how to decide on engineering change given a set of possible requirement changes $\Omega_R$ [11, 42, 13, 43, 44]. Several assumptions were made to simplify the analysis and obtain comparative numerical results.

We modeled every possible requirement change, by considering the parameters governing the requirement PDFs (the mean and standard deviation) to be random and uniformly distributed. We solved the optimization problem for every possible requirement arc to obtain a set of solutions. In practice, such exhaustive search strategies can be limited by relatively small computational budgets. We attempt to overcome this difficulty by using optimization and Monte-Carlo simulation coupled with an early stopping criterion (based on whether the design rankings in Figure 7 have stabilized) to explore the set $\Omega_R$ which represents all the possible requirement changes that can happen. The large cardinality of this set $(6 \times 10^{50})$ reflects this challenge.

Most engineering organizations have detailed change request records. Change propagation analysis based on existing documentation of change requests assists designers in understanding what requirement changes are likely to occur at different stages of the product development cycle [43,44] and within different subsystems of the design [11, 13, 43]. This information can be leveraged to reduce the set $\Omega_R$ to a manageable size (say only the 10000 most important changes) for the design margin analysis presented in this paper. Just as design margin analysis can benefit from change propagation analysis, our method can support the choice of rating scales (i.e., the optimality rankings we present in Figure 7) in an engineering change propagation analysis such as that provided by Koh et al. [13].

Our analysis assumed that the uncertain parameters

14                                                    Copyright © by ASME

Table 3: Set-based solution comparison

| Quantity | Set of feasible design alternatives $\Omega_{cD}$ | | Set of robust design alternatives $S_R$ | | Set of flexible design alternatives $S_F$ | | Set of optimal design alternatives $S_E$ | |
|---|---|---|---|---|---|---|---|---|
| | $W$ | $V_c$ | $W$ | $V_c$ | $W$ | $V_c$ | $W$ | $V_c$ |
| Lower | 4.32 | 0.059 | 15.66 | 0.992 | 4.32 | 0.127 | 11.47 | 0.736 |
| Upper | 26.74 | 1.00 | 26.74 | 1.00 | 11.28 | 0.812 | 24.70 | 1.00 |
| Set centroid | 14.02 | 0.533 | 22.34 | 0.998 | 6.86 | 0.492 | 16.35 | 0.920 |
| $V_{\text{hyper-rectangle}}$ | 1 | | 0.0038 | | 0.226 | | 0.166 | |
| $V_{\text{convhull}}$ | 0.758 | | 0.0026 | | 0.092 | | 0.104 | |
| $\%V_{\text{feasible}}$ | 75.8% | | 0.26% | | 9.2% | | 10.4% | |
| $D_{\text{Pareto}}$ | 0.421 | | 0.298 | | 0.172 | | 0.0904 | |
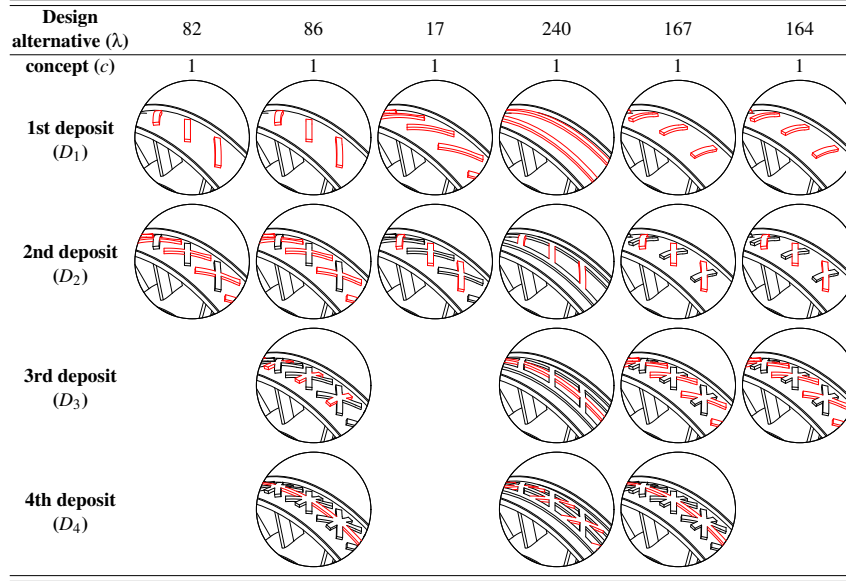


Fig. 9: Top performing design alternatives in $S_E$

$T_1, T_2, T_3$, and $T_4$ are uncorrelated (i.e., the off-diagonal terms of the covariance matrix $\Sigma$ in Equation (5) are equal to zero) when formulating a requirement. This assumption was made due to the lack of operational data needed to estimate the covariance matrix and to simplify the computation of the reliability integral. A second-order DSM approach for managing requirement changes is particularly useful for identifying those correlations since it shares the same size and features with the covariance matrix [11].

The analysis presented in this paper is restricted to the allocation of design margins on a single component, the TRS. Engineering change can span complex product systems with multiple subsystems [11, 13, 43]. The design margins of several interacting components should be considered simultaneously and formulations for such system-level design margins are provided in the literature [2, 45].

The optimization in Equation (24) uses "cumulative excess" as the objective function. This has the effect of penalizing carrying a large amount of excess in epoch 1. If we consider re-design of a product or system that is already in operation, accumulating excess early in the product's life will lead to greater weight which translates to an accumulation of running costs due to the increased fuel consumption associated with the added weight [46]. Furthermore, minimization of excess is only possible in the early design stages when requirements are still fluid. The high reliability threshold towards the end of the design process (see Figure 5a) restricts the minimization of excess. An additional constraint can be added to the optimization problem to ensure a certain minimum amount of excess is built into the design throughout the design process. The safety factor threshold in Equation (34) can be increased to provide an added layer of safety. The reliability thresholds could also be revised at the start of every epoch based on the current circumstances of the industry or project (e.g., new industrial standards) to give more accurate estimates of reliability and excess.

Different objectives such as life-cycle cost, weight, or stiffness can be used in lieu of excess and the resulting sets of solutions can all be compared in a tradespace to gain more insight about possible competing objectives. Alternatively, different objectives can be aggregated via a weighted sum based on designer preferences. The set of solutions based on this aggregate objective function reflects those preferences.

The decision making problem given by Equation (24)

assumes that repeated change decisions are not possible. This stems from manufacturing constraints specific to the re-manufacturing application in this paper. This constraint can be relaxed for other manufacturing methods such as conventional machining to recall a change. The extended poll used to define the categorical neighborhood of different decisions can be changed to allow repetition if necessary. A penalty could be associated with such a change to discourage the optimizer from retracting changes. This is because repetition of changes (whether by AM or not) is not reversible in most cases and involves a kind of "friction" when reverting the change.

This paper does not consider the effect of new or disruptive technological solutions. Such considerations can be incorporated as a design alternative that provides an extremely high capability (as well as buffer and excess by proxy) but at a high cost due to low maturity (given by technology readiness level) [2]. This definition can be adopted when attempting to include change options that represent such experimental design choices in future work.

## 7 Conclusion

We presented a method for the strategic allocation of design margins to cope with changing requirements of a system and its components. Design arcs are obtained by solving an optimization problem to minimize excess subject to reliability constraints that reflect such changing requirements.

The proposed method allows designers to identify several candidate design alternatives to develop concurrently with potential to evolve and satisfy a wide range of requirement change scenarios without risking overdesigning the product. Such insights are particularly useful to designers in the early stages of product development when little information regarding the requirements or their future values is available. The tools and methods developed in this paper are publicly available on a code repository (GitHub, https://github.com/khbalhandawi/DM_SBD_opt).

Furthermore, our tradespace exploration strategy helps designers position the candidate design alternatives relative to other widely used strategies such as design for flexibility or robustness. This is useful for narrowing down the set of candidate solutions depending on the preference of designers for flexibility or robustness. Finally, designers can identify solutions that may otherwise be overlooked when only considering Pareto optimal designs from a tradespace obtained from information at a particular time in the development cycle.

In our methodology, we considered a feasible set that consists of permutations of discrete design choices. More alternatives can be discovered by considering a continuous or mixed variable design space. More advanced importance sampling methods can be used for determining the volumes of excess and capability in the multi-dimensional parameter space. Other more representative tradespace attributes can be used to denote the utility or cost of a design such as lifecycle cost.

The novel design margin metrics and corresponding al-

location strategy presented in this work provide designers with the tools necessary to achieve designs that can endure the long lifecycles expected in the aerospace industry.

## References

[1] C. Peterson, R. K. Paasch, P. Ge, and T. G. Dietterich. Product innovation for interdisciplinary design under changing requirements. In *Proceedings of the International Conference on Engineering Design*, pages 861–862, Paris, 2007.

[2] C. Eckert, O. Isaksson, and C. Earl. Design margins: A hidden issue in industry. *Design Science*, 5:e9, 2019.

[3] D. Long and S. Ferguson. A case study of evolvability and excess on the B-52 stratofortress and F/A-18 hornet. In *Proceedings of the ASME International Design Engineering Technical Conferences and Computers and Information in Engineering Conference*, volume 4. American Society of Mechanical Engineers (ASME), 2017.

[4] D. Ullman. *The mechanical design process*. McGraw-Hill. McGraw-Hill Education, 2009.

[5] W. L. Ijomah. Addressing decision making for remanufacturing operations and design-for-remanufacture. *International Journal of Sustainable Engineering*, 2(2):91–102, 2009.

[6] W. Ijomah, C. McMahon, G. Hammond, and S. Newman. Development of robust design-for-remanufacturing guidelines to further the aims of sustainable development. *International Journal of Production Research*, 45(18-19):4513–4536, 2007.

[7] P. Golinska, M. Kosacka, R. Mierzwiak, and K. Werner-Lewandowska. Grey decision making as a tool for the classification of the sustainability level of remanufacturing companies. *Journal of Cleaner Production*, 105:28–40, 2015.

[8] R. G. Cooper. Perspective: The stage-gates® idea-to-launch process - Update, what's new, and NexGen systems. *Journal of Product Innovation Management*, 25(3):213–232, 2008.

[9] H. L. Mcmanus, M. G. Richards, A. M. Ross, and D. E. Hastings. A framework for incorporating "ilities" in tradespace studies. In *Proceedings of the AIAA SPACE 2007 Conference & Exposition*, 2007.

[10] P. J. Clarkson, C. Simons, and C. Eckert. Predicting change propagation in complex design. *Journal of Mechanical Design*, 126(5), 2004.

[11] B. Morkos, P. Shankar, and J. D. Summers. Predicting requirement change propagation, using higher order design structure matrices: an industry case study. *Journal of Engineering Design*, 23(12):905–926, 2012.

[12] B. Morkos and J. D. Summers. Requirement change propagation prediction approach: Results from an industry case study. In *Proceedings of the ASME Design Engineering Technical Conference*, volume 1, pages 111–121. American Society of Mechanical Engineers Digital Collection, mar 2010.

[13] E. C.Y. Koh, N. H.M. Caldwell, and P. J. Clarkson. A method to assess the effects of engineering change propagation. *Research in Engineering Design*, 23(4):329–351, oct 2012.

[14] M. W. P. Tackett, C. A. Mattson, and S. M. Ferguson. A model for quantifying system evolvability based on excess and capacity. *Journal of Mechanical Design*, 136(5), 2014.

[15] E. Z. Cansler, S. B. White, S. M. Ferguson, and C. A. Mattson. Excess identification and mapping in engineered systems. *Journal of Mechanical Design*, 138(8), 2016.

[16] C. F. Rehn, S. S. Pettersen, S. O. Erikstad, and B. E. Asbjørnslett. Investigating tradeoffs between performance, cost and flexibility for reconfigurable offshore ships. *Ocean Engineering*, 147:546–555, 2018.

[17] M. A. Cardin, Q. Xie, T. S. Ng, S. Wang, and J. Hu. An approach for analyzing and managing flexibility in engineering systems design based on decision rules and multistage stochastic programming. *IISE Transactions*, 49(1):1–12, 2017.

[18] P. L. Cross and M. Mulford. Realizing collaborative systems design for missile seekers by combining design margin analysis with multi-disciplinary optimization. *Concurrent Engineering Research and Applications*, 23(3):226–235, 2015.

[19] D. Villanueva, R. T. Haftka, and B. V. Sankar. Accounting for future redesign to balance performance and development costs. *Reliability Engineering and System Safety*, 124:56–67, 2014.

[20] S. Rapp, R. Chinnam, N. Doerry, A. Murat, and G. Witus. Product development resilience through set-based design. *Systems Engineering*, 21(5):490–500, 2018.

[21] M. A. Cardin and J. Hu. Analyzing the tradeoffs between economies of scale, time-value of money, and flexibility in design under uncertainty: study of centralized versus decentralized waste-to-energy systems.

[22] A. Ross, D. Rhodes, and D. E. Hastings. Defining changeability: Reconciling flexibility, adaptability, scalability, modifiability, and robustness for maintaining system lifecycle value. *Systems Engineering*, 11(3):246–262, 2008.

[23] E. Fricke and A. P. Schulz. Design for changeability (DfC): Principles to enable changes in systems throughout their entire lifecycle. *Systems Engineering*, 8(4):342–359, 2005.

[24] M. J. Chalupnik, D. C. Wynn, and P. J. Clarkson. Comparison of ilities for protection against uncertainty in system design. *Journal of Engineering Design*, 24(12):814–829, 2013.

[25] L. Viscito and A. Ross. Quantifying flexibility in tradespace exploration: Value-weighted filtered outdegree. In *Proceedings of the AIAA SPACE 2009 Conference & Exposition*, Pasadena, California, 2009. American Institute of Aeronautics and Astronautics.

[26] C. Small, G. S. Parnell, E. Pohl, S. R. Goerger, M. Cilli, and E. Specking. Demonstrating set-based design techniques: an unmanned aerial vehicle case study. *Journal of Defense Modeling and Simulation*, pages 1–17, 2019.

[27] H. J. Pradlwarter, M. F. Pellissetti, C. A. Schenk, G. I. Schuëller, A. Kreis, S. Fransen, A. Calvi, and M. Klein. Realistic and efficient reliability estimation for aerospace structures. *Computer Methods in Applied Mechanics and Engineering*, 194(12-16):1597–1617, 2005.

[28] D. M. Frangopol and K. Maute. Life-cycle reliability-based optimization of civil and aerospace structures. *Computers and Structures*, 81(7):397–410, 2003.

[29] S. Zhu, H. Huang, R. Smith, V. Ontiveros, L. He, and M. Modarres. Bayesian framework for probabilistic low cycle fatigue life prediction and uncertainty modeling of aircraft turbine disk alloys. *Probabilistic Engineering Mechanics*, 34:114–122, 2013.

[30] A. F. Shahraki and R. Noorossana. Reliability-based robust design optimization: A general methodology using genetic algorithm. *Computers & Industrial Engineering*, 74:199–207, 2014.

[31] C. Bucher. *Computational analysis of ramdomness in structural mechanics*. CRC Press, 2009.

[32] P. E. Magnusen, R. J. Bucci, A. J. Hinkle, J. R. Brockenbrough, and H. J. Konish. Analysis and prediction of microstructural effects on long-term fatigue performance of an aluminum aerospace alloy. *International Journal of Fatigue*, 19(93):275–283, 1997.

[33] M. Zhang, W. Gou, L. Li, X. Wang, and Z. Yue. Multidisciplinary design and optimization of the twin-web turbine disk. *Structural and Multidisciplinary Optimization*, 53(5):1129–1141, 2016.

[34] M. Kleiber, J. Knabel, and J. Rojek. Response surface method for probabilistic assessment of metal forming failures. *International Journal for Numerical Methods in Engineering*, 60(1):51–67, 2004.

[35] M. A. Abramson, C. Audet, J. W. Chrissis, and J. G.

Walston. Mesh adaptive direct search algorithms for mixed variable optimization. *Optimization Letters*, 3(1):35–47, 2009.

[36] M. A. Abramson. Mixed variable optimization of a load-bearing thermal insulation system using a filter pattern search algorithm. *Optimization and Engineering*, 5(2):157–177, 2004.

[37] M. A. Abramson, T. J. Asaki, J. E. Dennis, K. R. O'Reilly, and R. L. Pingel. Quantitative object reconstruction using abel transform X-ray tomography and mixed variable optimization. *SIAM Journal on Imaging Sciences*, 1(3):322–342, 2008.

[38] K. Alhandawi, P. Andersson, M. Panarotto, O. Isaksson, and M. Kokkolaras. Scalable set-based design optimization and remanufacturing for meeting changing requirements. *Journal of Mechanical Design*, 143(2), 2020.

[39] U.S. Army Materiel Command. *Engineering design handbook: Automotive series-bodies and hulls*. 1970.

[40] B. Talgorn, C. Audet, S. Le Digabel, and M. Kokkolaras. Locally weighted regression models for surrogate-assisted design optimization. *Optimization and Engineering*, 19(1):213–238, 2018.

[41] N. Brown and C. Mueller. Quantifying diversity in parametric design: A comparison of possible metrics. *Artificial Intelligence for Engineering Design, Analysis and Manufacturing*, 33(1):40–53, 2019.

[42] P. Shankar, J. D. Summers, and K. Phelan. A verification and validation planning method to address change propagation effects in engineering design and manufacturing. *Concurrent Engineering Research and Applications*, 25(2):151–162, jun 2017.

[43] M. Giffin, O. De Weck, G. Bounova, R. Keller, C. Eckert, and P. J. Clarkson. Change propagation analysis in complex technical systems. *Journal of Mechanical Design, Transactions of the ASME*, 131(8):0810011–08100114, aug 2009.

[44] L. Almefelt, F. Berglund, P. Nilsson, and J. Malmqvist. Requirements management in practice: Findings from an empirical study in the automotive industry. *Research in Engineering Design*, 17(3):113–134, dec 2006.

[45] C. Eckert, O. Isaksson, S. Lebjioui, C. F. Earl, and S. Edlund. Design margins in industrial practice. *Design Science*, 6, 2020.

[46] L. Lawand, M. Panarotto, P. Andersson, O. Isaksson, and M. Kokkolaras. Dynamic lifecycle cost modeling for adaptable design optimization of additively remanufactured aeroengine components. *Aerospace*, 7(8):110, jul 2020.